



# Focal-type, but not Diffuse-type, Amyloid Beta Plaques are Correlated with Alzheimer's Neuropathology, Cognitive Dysfunction, and Neuroinflammation in the Human Hippocampus

Fan Liu<sup>1,2</sup> · Jianru Sun<sup>2</sup> · Xue Wang<sup>1,2</sup> · Sixuan Jin<sup>2</sup> · Fengrun Sun<sup>2</sup> · Tao Wang<sup>2</sup> · Bo Yuan<sup>2</sup> · Wenying Qiu<sup>1,2</sup> · Chao Ma<sup>1,2,3</sup>

Received: 18 December 2021 / Accepted: 28 April 2022 / Published online: 26 August 2022  
© The Author(s) 2022

**Abstract** Amyloid beta (A $\beta$ ) plaques are one of the hallmarks of Alzheimer's disease (AD). However, currently available anti-amyloid therapies fail to show effectiveness in the treatment of AD in humans. It has been found that there are different types of A $\beta$  plaque (diffuse and focal types) in the postmortem human brain. In this study, we aimed to investigate the correlations among different types of A $\beta$  plaque and AD-related neuropathological and cognitive changes based on a postmortem human brain bank in China. The results indicated that focal plaques, but not diffuse plaques, significantly increased with age in the human hippocampus. We also found that the number of focal plaques was positively correlated with the severity of AD-related neuropathological changes (measured by the "ABC" scoring system) and cognitive decline (measured by the Everyday Cognitive Insider Questionnaire). Furthermore, most of the focal plaques were co-localized with neuritic plaques (identified

by Bielschowsky silver staining) and accompanied by microglial and other inflammatory cells. Our findings suggest the potential of using focal-type but not general A $\beta$  plaques as biomarkers for the neuropathological evaluation of AD.

**Keywords** Focal A $\beta$  plaques · ECog score · ABC score · Alzheimer's disease · Neuroinflammation · Clinicopathological correlation · Human brain bank

## Introduction

Alzheimer's disease (AD) causes prolonged suffering in patients and societal issues. Amyloid-beta (A $\beta$ ) deposits, neurofibrillary tangles (NFTs), and neuritic plaques (NPs) are the hallmark pathologic findings in the brains of AD patients [1]. A $\beta$ , produced by the sequential cleavage of  $\beta$ -amyloid precursor protein through  $\beta$ -secretase and  $\gamma$ -secretase, is released from neurons through both presynaptic and postsynaptic modulation [2–5]. NPs are pathological structures containing A $\beta$  along with neural and microglial elements. Dystrophic neural processes containing aggregated, phosphorylated tau surrounding A $\beta$  deposits are a key feature of NPs [6]. Toxic A $\beta$  deposits evoke a cascade of oxidative damage-dependent apoptosis in neurons [7–9]. Earlier studies have shown that the accumulation of A $\beta$  plaques enhances the formation of NFTs and NPs, and this may be necessary for the progression of tau pathology in AD [10–12]. Although the amyloid cascade hypothesis seems to be that A $\beta$  plays a key role in AD [10, 13–15], until now, therapies involving anti-A $\beta$  treatments, including A $\beta$ -directed monoclonal antibodies, A $\beta$  vaccines, A $\beta$  aggregation inhibitors and  $\beta$ -secretase inhibitors, have failed in clinical trials [16, 17].

Current anti-A $\beta$  treatments for AD are poorly effective, owing to limited knowledge of the pathophysiological

Fan Liu and Jianru Sun have contributed equally to this work.

**Supplementary Information** The online version contains supplementary material available at <https://doi.org/10.1007/s12264-022-00927-5>.

✉ Chao Ma  
machao@ibms.cams.cn

<sup>1</sup> National Human Brain Bank for Development and Function, School of Basic Medicine Peking Union Medical College, Institute of Basic Medical Sciences Chinese Academy of Medical Sciences, Beijing 100005, China

<sup>2</sup> Department of Human Anatomy, Histology and Embryology, Neuroscience Center, School of Basic Medicine Peking Union Medical College, Institute of Basic Medical Sciences Chinese Academy of Medical Sciences, Beijing 100005, China

<sup>3</sup> Chinese Institute for Brain Research, Beijing 102206, China

mechanisms underlying A $\beta$  [10, 17–20]. Some studies have reported a lack of correlation between A $\beta$  plaques and cognitive decline in AD patients [20–22]. Based on the postmortem neuropathological diagnosis of AD, some studies have found that A $\beta$  is also widely present in the elderly human brain with normal cognition [23]. PET imaging studies found small amounts of A $\beta$  deposition in the brains of some diagnosed AD patients [24, 25]. Recently, more studies have suggested that A $\beta$  has multiple physiological functions, such as the regulation of learning and memory, angiogenesis, and neurogenesis, and the promotion of recovery from injury [18, 19].

A $\beta$  peptides of different lengths can transform into oligomeric and fibril forms and eventually form amyloid plaques [2, 18, 19]. Much research has strongly suggested that A $\beta$ , ranging from soluble oligomers to insoluble fibrils and plaques, causes and leads to the pathogenic cascade of AD [26]. The A $\beta$ 42 peptide has been found to be more neurotoxic and more prone to aggregation than the A $\beta$ 40 peptide [27, 28]. Many studies have also reported that A $\beta$  oligomers are more neurotoxic than plaques and can lead to cognitive deficits [29]. Based on postmortem neuropathology of the human brain, A $\beta$  plaques have different morphological forms, which are mainly classified into diffuse and focal (or dense-core) types [30–32]. Diffuse A $\beta$  plaques are seen on immunostaining as loose structures with irregular, ill-defined margins, while focal A $\beta$  plaques have clear-cut outlines and generally have a core [32]. Although electron microscopic analysis of the postmortem human brain has shown that all forms of A $\beta$  plaque are associated with neuropathology, there are significant differences between diffuse and focal A $\beta$  plaques [33, 34]. Previous studies revealed that focal A $\beta$  plaques may cause neuronal damage and microglial activation, which are closely associated with the pathological changes of AD [30, 31].

AD patients undergo progressive A $\beta$  plaque deposition followed by surrounding neuritic and glial cytopathology in the brain [31, 35]. The accumulation of toxic forms of A $\beta$  affects synaptic function and plasticity and triggers glial activation and neuroinflammation [35]. However, it is not fully clear which specific A $\beta$  plaque type is involved. Here, we explore the correlation among different A $\beta$  plaque forms, brain pathology, clinical cognition, and neuroinflammation based on cases from the National Human Brain Bank for Development and Function, Institute of Basic Medical Sciences, Chinese Academy of Medical Sciences.

## Materials and Methods

### Human Brain Sample Sources

A total of 92 human brain samples fixed in 10% formalin from the National Human Brain Bank for Development and Function, Institute of Basic Medical Sciences, Chinese Academy of Medical Sciences, were used in this research.

Detailed information, including demographic variables, ABC scores, ECog scores, and other information on all donors, are listed in Table S1. The research protocol was approved by the Institutional Review Board of the Institute of Basic Medical Sciences of the Chinese Academy of Medical Sciences, China (Approval Numbers: 009–2014 and 031–2017).

### Neuropathological Evaluation

According to the guidelines of the National Institute on Aging and Alzheimer's Association (NIA-AA), all brain tissue received identical neuropathological analysis by the "ABC" score, which was performed by a brain bank professional. The ABC score incorporates amyloid- $\beta$  (A $\beta$ ) deposits (A Score), neurofibrillary tangles (B Score), and neuritic plaques (C Score). The A score reflects the order of amyloid- $\beta$  appearance in the brain in a tiered manner, but the specific plaque type is not distinguished [36]. The general ABC score is categorized into 4 grades of AD neuropathological change: none (N), low (L), intermediate (I), and high (H). A neuropathological AD score of N/L indicates that the donor is unlikely to have AD and can be regarded as a normal elderly person. A neuropathological AD score of I/H indicates that the donor is very likely to have AD and can be considered a sufficient explanation for dementia [36]. Among 92 A $\beta$ -positive brain tissue donors, 19 had AD neuropathological scores that were L, and 73 were I/H, which were very likely to have AD. The detailed pathological information of each case is listed in Table S1.

### Cognitive Function Assessment

Of the 92 human brain samples, only 84 had ECog scores. Clinical cognitive status was determined using the Everyday Cognitive (ECog) Insider Questionnaire, which includes 39 questions aimed to assess the daily cognitive function of the brain donors. And there are 6 sub-items (memory, language, visuospatial functions, planning, organization, and divided attention) in the ECog questionnaire [37, 38]. In accordance with the criteria for ECog scores, normal cognition was defined as an ECog score  $\leq 1.0$ , mild cognitive impairment as an ECog score 1.0–2.0, and dementia as an ECog score  $> 2.0$ .

### Immunohistochemistry and Immunofluorescence Staining

Based on the NIA-AA guidelines, these brain regions (superior frontal cortex, primary motor cortex, inferior temporal

cortex, hippocampus, anterior cingulate cortex, amygdala, supramarginal cortex, caudate/putamen, midbrain, pons, medulla oblongata, and cerebellar dentate nucleus) were sampled from postmortem human brains and brain tissues were embedded in paraffin. Given that A $\beta$  plaques are stereoscopic and that the top view of a plaque would differ from the middle and bottom views, we applied serial section staining to compensate for this drawback. Specifically, we randomly selected one sample in which the ABC score was "I" and had a certain number of focal plaques and diffuse plaques. Then, five paraffin sections were cut at 5  $\mu$ m continuously for A $\beta$  immunohistochemical staining. We randomly selected 4 visual fields. For each section, we judged the subtype of each A $\beta$  plaque in the 4 fields. The actual subtype of each A $\beta$  plaque was judged by synthesizing five sections. Then, we calculated the accuracy of plaque judgment for each section to finally obtain the average accuracy. To study the co-localization of A $\beta$  plaques and NPs, 5 human brain hippocampi covering the "L/I/H" group were serially sectioned, and the adjacent sections were subjected to A $\beta$  immunohistochemical staining and modified Bielschowsky for NPs.

In staining for pathological A and B scoring, the paraffin-embedded brain samples were cut at 5  $\mu$ m, and for C scoring at 10  $\mu$ m. The staining for the A and B scores was based on immunohistochemistry against  $\beta$ -amyloid (mouse monoclonal antibody, diluted 1:200, DAKO Cat#M0872) and p-Tau (Ser202, Thr205) (p-Tau, mouse monoclonal antibody, 1:800, Thermo Cat#MN1020). The method for A $\beta$  deposits was immunohistochemistry for A $\beta$ , and for NFTs, the method was immunohistochemistry for p-Tau (Ser202, Thr205) [21]. The primary antibodies were incubated separately overnight at 4°C and then processed for 60 min with a mouse two-step detection kit (mouse enhanced polymer detection system; ZSGB-BIO PV-9002, Beijing, China). The staining results were visualized with a DAB chromogenic kit (ZSGB-BIO ZLI-9019, Beijing, China). The C score was determined by modified Bielschowsky staining for neuritic processes in senile plaques [39].

Formalin-fixed hippocampal tissue was embedded in OCT medium (Sakura) and then cut at 16  $\mu$ m on a cryostat for immunofluorescent staining. Double immunofluorescence staining was used for co-labeling of A $\beta$  and IBA1. For the co-labeling of A $\beta$  and CD68, CD86, or CD19, the same section was used prior to A $\beta$  immunohistochemistry, followed by immunofluorescence staining for the CD molecule. The frozen sections were incubated separately overnight at 4°C in primary antibodies (rabbit anti-IBA1, 1:200, Abcam Cat#ab178846; mouse anti-CD68, 1:1000, Abcam Cat#ab955; rabbit anti-CD86, 1:200, Cell Signaling Technology Cat#91882S; rabbit anti-CD19, 1:800, Cell Signaling Technology Cat#90176T; rabbit anti-A $\beta$ , 1:200, Abcam Cat#ab2539; mouse anti-A $\beta$ , 1:200, DAKO Cat#M0872) and

then incubated with the appropriate secondary antibodies (Alexa Fluor 594-conjugated goat anti-rabbit, 1:400; Alexa Fluor 488-conjugated goat anti-mouse, 1:500; HRP-conjugated goat anti-mouse, 1:500; or HRP-conjugated goat anti-rabbit, 1:500). DAB reagent was added after incubation with HRP-conjugated secondary antibodies. The slides were then washed in PBS and cover-slipped with Vectashield mounting medium with DAPI. Images of the sections were captured using a microscopic imaging system (Olympus BX61 and FluoView software).

Immunohistochemistry against A $\beta$  was analyzed in ten 10 $\times$  microscopic fields using ImageScope software from a similar position in human brain hippocampus sections, including CA1-CA4, subiculum, and entorhinal cortex, and the actual tissue area observed was 20 mm<sup>2</sup>. The summation represented the number of A $\beta$  plaques. We divided A $\beta$  plaques into two types: diffuse and focal. Plaques looking like loose structures with irregular and ill-defined margins were defined as diffuse; and plaques that had clear-cut outlines and generally had a compact core or strong sepia granular texture were defined as focal. Then, the percentage of each plaque type can be calculated.

## Statistical Analysis

Values are expressed as the mean  $\pm$  SEM. Statistical analyses were conducted using SPSS software (version 17.0) and GraphPad software. Student's *t* test was used to analyze the statistical significance of differences between 2 groups, and one-way analysis of variance (ANOVA) followed by Scheffe's *post-hoc* test was used to analyze the statistical significance of differences among 3 groups. The relationship between different types of data was analyzed with Spearman correlation analysis. *P* < 0.05 was considered significant.

## Results

### Association Between Hippocampal A $\beta$ Plaque Forms and Demographic Variables

IHC results revealed that hippocampal A $\beta$  plaques existed in different forms in A $\beta$  plaque-positive human brain samples (Fig. 1). The two most common subtypes, diffuse and focal A $\beta$  plaques, were classified according to their unique appearance in hippocampal tissue. Diffuse A $\beta$  plaques were seen on immunostaining as loose structures with irregular, ill-defined margins, while focal A $\beta$  plaques had clear-cut outlines and generally had a core. Focal A $\beta$  plaques are extracellular proteinaceous deposits composed of A $\beta$  peptide, largely as amyloid filaments, while in diffuse plaques, the majority of the protein is not aggregated as amyloid filaments [32, 40]. It is important to further comprehend the differences between

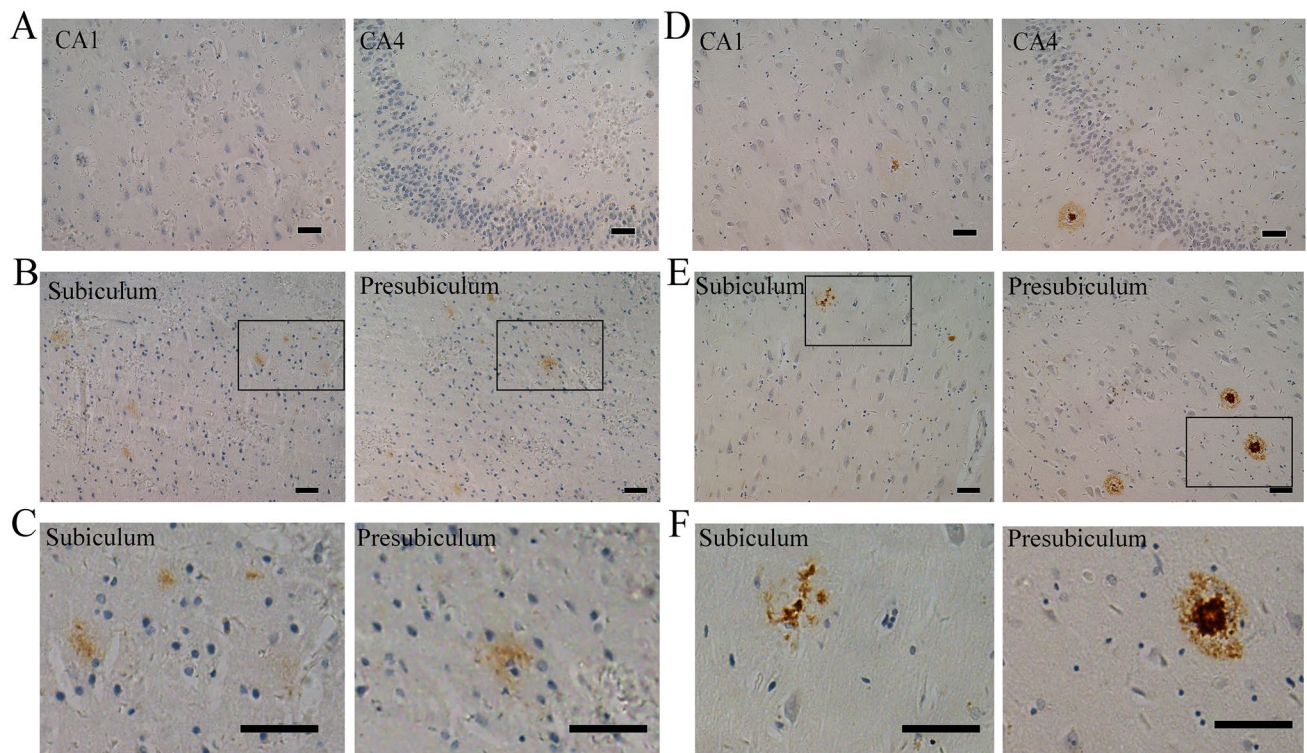


**Fig. 1** Histochemical staining showing the morphology of different forms of A $\beta$  plaque in the human hippocampus. **A, B** Diffuse A $\beta$  plaques in A $\beta$  plaque-positive hippocampal tissue. Negative A $\beta$  plaques in CA1 and CA4 (**A**) and positive diffuse A $\beta$  plaques in the subiculum and presubiculum (**B**) with an ABC score of “L”. **C** Enlarged image of diffuse A $\beta$  plaques in the subiculum and presub-

iculum. **D, E** Focal A $\beta$  plaques from A $\beta$  plaque-positive hippocampal tissue. Positive focal A $\beta$  plaques in CA1–CA4 (**D**), subiculum and presubiculum (**E**) with an ABC score of “H”. **F** Enlarged image of focal A $\beta$  plaques in the subiculum and presubiculum. Scale bars, 50  $\mu$ m in (A–F).

focal and diffuse plaques. Representative images of diffuse A $\beta$  plaques in hippocampal tissue from samples with an “L” ABC score are shown in Fig. 1A–C. Representative images of focal A $\beta$  plaques in the hippocampus from samples with an “H” ABC score are shown in Fig. 1D–F. Given that A $\beta$  plaques are stereoscopic, we used serial section staining to calculate the accuracy of morphological judgment through only one section. Through the overall interpretation of 5 consecutive sections, we concluded that there were 10 diffuse plaques and 10 focal plaques. The average accuracy of random sections was 89% (Fig. S1A–E).

The association of demographic variables with the total number of A $\beta$  plaques in the hippocampus was investigated. There was no significant difference in the total number by sex (Student’s *t* test,  $P > 0.05$ ) (Fig. S2A) or among the different age groups (one-way ANOVA,  $P > 0.05$ ) (Fig. S2C). The association of demographic variables with different forms of hippocampal A $\beta$  plaque was investigated. There was no significant difference in the numbers or percentages of diffuse or focal A $\beta$  plaques by sex (Student’s *t* test,  $P > 0.05$ ) (Fig. 2A–D). According to the age at death, Spearman rank correlation analysis showed no significant correlation

between the number and percentage of diffuse plaques and age (Fig. 2E, G). The number and percentage of focal plaques showed a significantly positive correlation with age (Fig. 2F, H). The human brain mass was also used to investigate the correlation between A $\beta$  plaques and brain atrophy. The results showed that the total number of A $\beta$  plaques in the hippocampus was not significantly correlated with brain mass (Fig. S3A). Neither the number of diffuse nor of focal plaques showed significant correlation with brain mass (Fig. S3B–C). This suggests that as age increases, focal A $\beta$  plaques in the human hippocampus tend to increase.

### Correlation Between Hippocampal A $\beta$ Plaque Forms and AD-related Neuropathological Changes

IHC experiments indicated that the number of diffuse A $\beta$  plaques did not significantly change in the hippocampus, while more focal A $\beta$  plaques were observed in the intermediate (“I” ABC score) or high-level (“H” ABC score) AD neuropathological brain samples (Fig. 3A). The assessment of samples was conducted according to ABC scores, which included A $\beta$  deposits, NFTs (p-Tau), and NPs. Fig. 3B

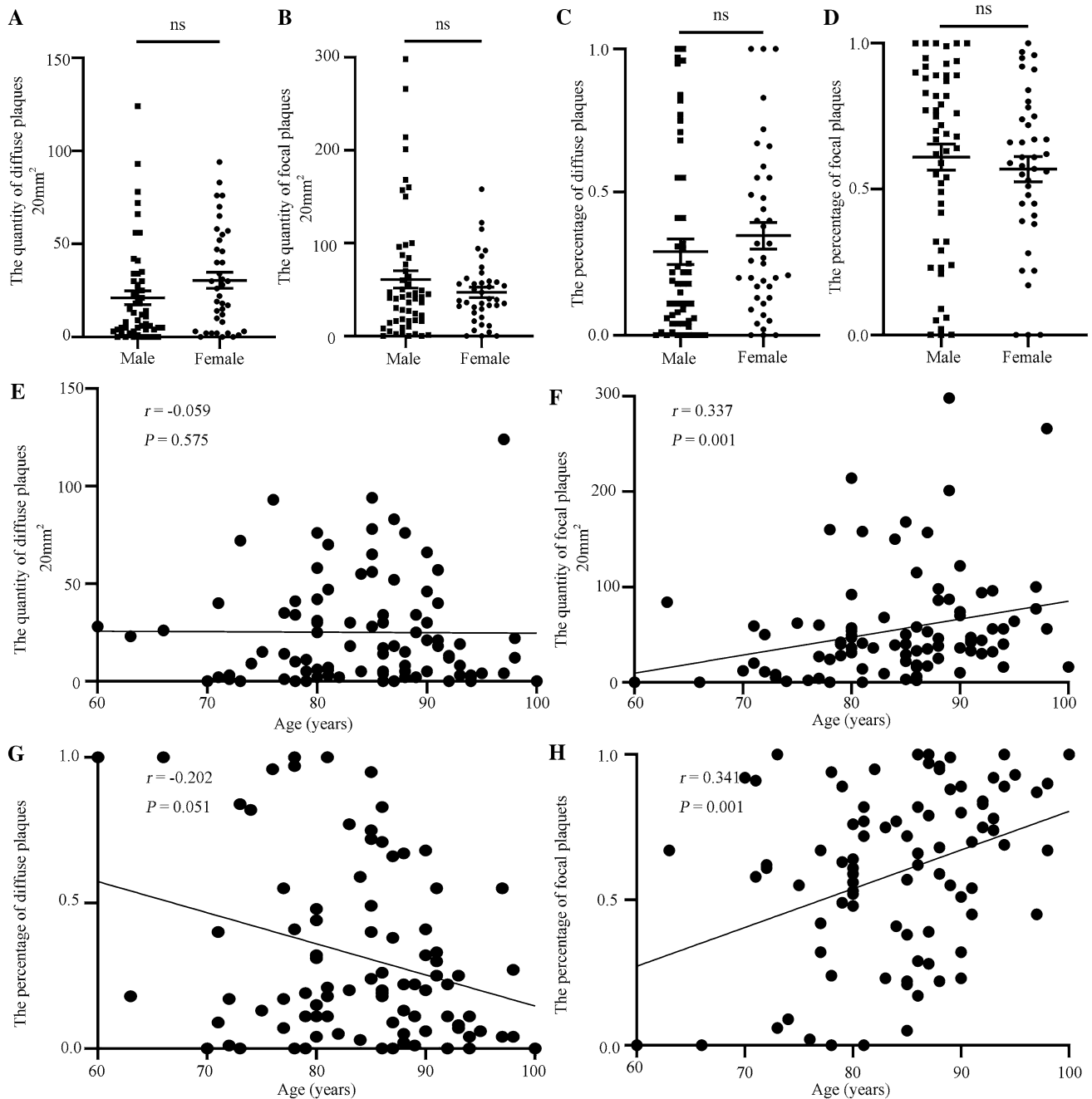


**Fig. 2** Correlation between demographic variables and A $\beta$  plaque forms. **A** Quantification of diffuse A $\beta$  plaques by gender. **B** Quantification of focal A $\beta$  plaques by sex. **C** Percentage of diffuse A $\beta$  plaques by sex. **D** Percentage of focal A $\beta$  plaques by sex. In (A–D), male = 53 samples, female = 39 samples, male group *versus* female group; *ns*, no significant difference, Student's *t* test. **E** Quantification of diffuse A $\beta$  plaques at different ages.  $P > 0.05$ , no significant correlation

by Spearman correlation. **F** Quantification of focal A $\beta$  plaques at different ages.  $P = 0.001$ ,  $r = 0.337$ , significant positive correlation by Spearman correlation. **G** Percentage of diffuse A $\beta$  plaques at different ages.  $P > 0.05$ , no significant correlation by Spearman correlation. **H** Percentage of focal A $\beta$  plaques at different ages.  $P = 0.001$ ,  $r = 0.341$ , significant positive correlation by Spearman correlation.

shows immunohistochemical images of A $\beta$  plaques, p-Tau, and NPs in groups with different ABC scores. One-way ANOVA revealed that the total number of A $\beta$  plaques in the “I” and “H” score groups was significantly greater than that in the “L” group (Fig. 3C). Further analysis indicated

that the number of focal plaques, but not diffuse plaques, was significantly different among the different ABC score groups in the hippocampus (Fig. 3D–E). The number of focal plaques in the “I” and “H” groups was significantly greater than that in the “L” group (Fig. 3E). The samples

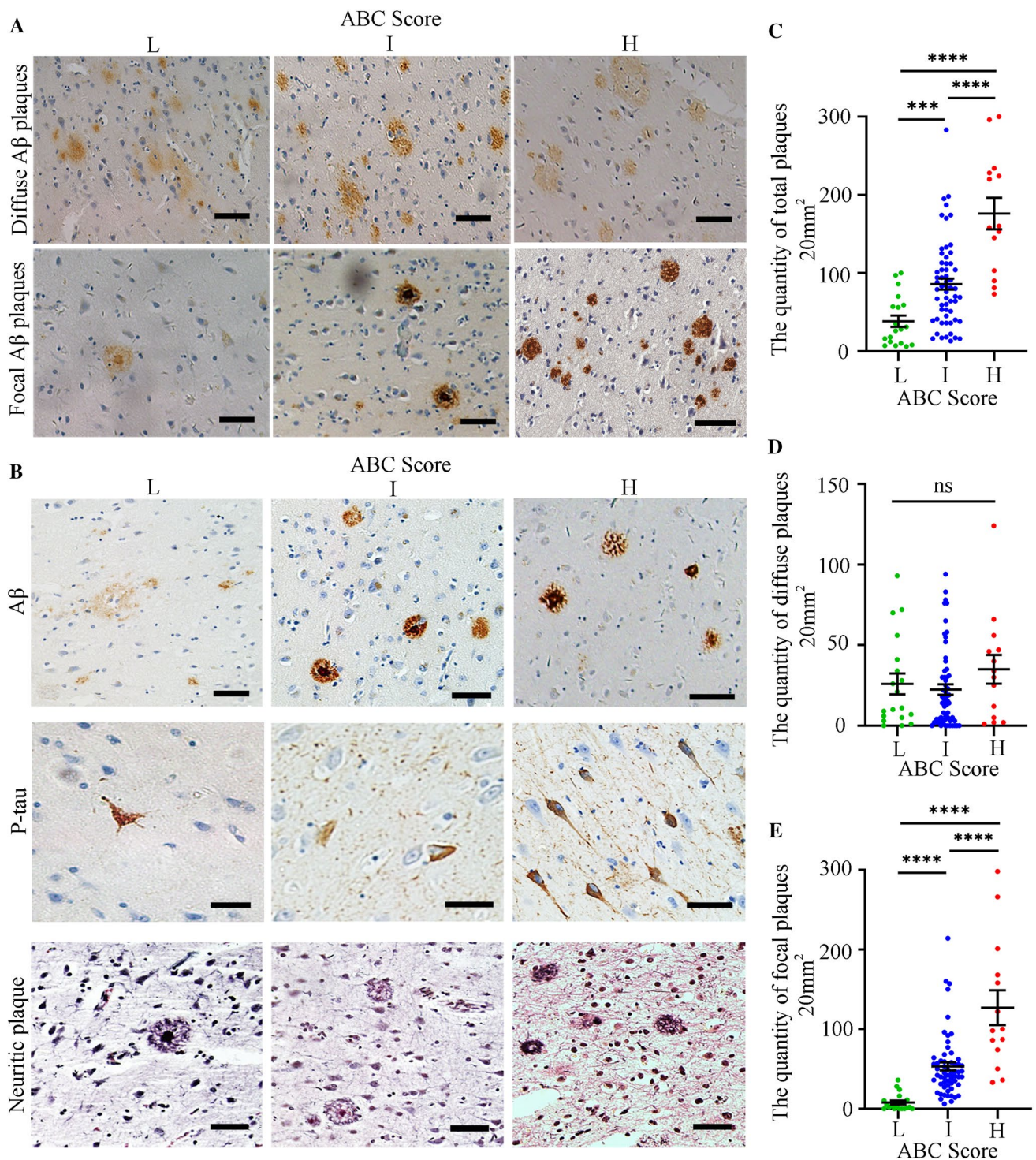


**Fig. 3** The number of hippocampal focal Aβ plaques increases with the degree of AD neuropathological change. **A** Distribution of diffuse and focal Aβ plaques in the hippocampus with different ABC scores of the human brain. **B** Neuropathological assessment of ABC score for Aβ plaque-positive human brain. In (**A**, **B**), scale bars, 50 μm. **C** The total number of Aβ plaques in the hippocampus from dif-

ferent ABC score groups. **D** Numbers of diffuse Aβ plaques in the hippocampus from different ABC score groups. **E** Numbers of focal Aβ plaques in the hippocampus from different ABC score groups. In (**C**–**E**), L group has 19 samples, I group has 59 samples, and H group has 14 samples, \*\*\* $P < 0.001$ , \*\*\*\* $P < 0.0001$ , ns, no significant difference by one-way ANOVA followed by Scheffe's *post-hoc* test.

were serially sectioned, and adjacent sections were subjected to A $\beta$  immunohistochemical staining and modified Bielschowsky for NPs. In the normal and AD group, diffuse plaques stained by immunohistochemistry and NPs stained by modified Bielschowsky showed almost no coincidence (Fig. 4A, B). However, the staining results showed that focal plaques coincided with NPs (Fig. 4C). We randomly counted 74 NPs from 5 hippocampi covering the “L/I/H” groups. The results showed that 71.6% of NPs coincided with focal A $\beta$  plaques and 23.0% of NPs coincided with diffuse A $\beta$  plaques (Fig. 4D). Randomly counting 88 diffuse plaques and 74 NPs from 5 hippocampi covering the “L/I/H” groups, showed only 11.4% diffuse plaques coincided with NPs and 13.5% of NPs coincided with diffuse plaques (Fig. 4E). After randomly counting 88 focal A $\beta$  plaques and 74 NPs from 5 hippocampi covering the “L/I/H” groups, 70.5% of focal plaques coincided with NPs, and 83.8% of NPs coincided with focal plaques (Fig. 4F).

Spearman rank correlation analysis showed no significant correlation between the number of diffuse plaques and ABC

score, B score, and C score (Fig. 5A–C); however, they were all moderately positive (Fig. 5D–F). It seems that focal A $\beta$  plaques, rather than diffuse plaques, play an important role in the neuropathological changes of AD. We made further efforts to evaluate the relationship between the percentage of each plaque type and AD neuropathological changes. One-way ANOVA revealed that the percentage of diffuse plaques in the “I” and “H” groups was significantly lower than that in the “L” group (Fig. 5G). Conversely, the percentage of focal plaques in the “I” and “H” groups was significantly greater than that in the “L” group (Fig. 5K). Spearman rank correlation analysis revealed that the correlation between diffuse plaque percentage and ABC score and B score was significantly negative for low intensity (Fig. 5H, I), while the percentage of focal plaques was significantly positively correlated with both ABC score and B score (Fig. 5L, M). We did not obtain significant results between the percentage of diffuse and focal plaques and the C score (Fig. 5J, N). The above results further suggest that focal A $\beta$  plaques, rather than diffuse plaques, participate in AD neuropathological changes.

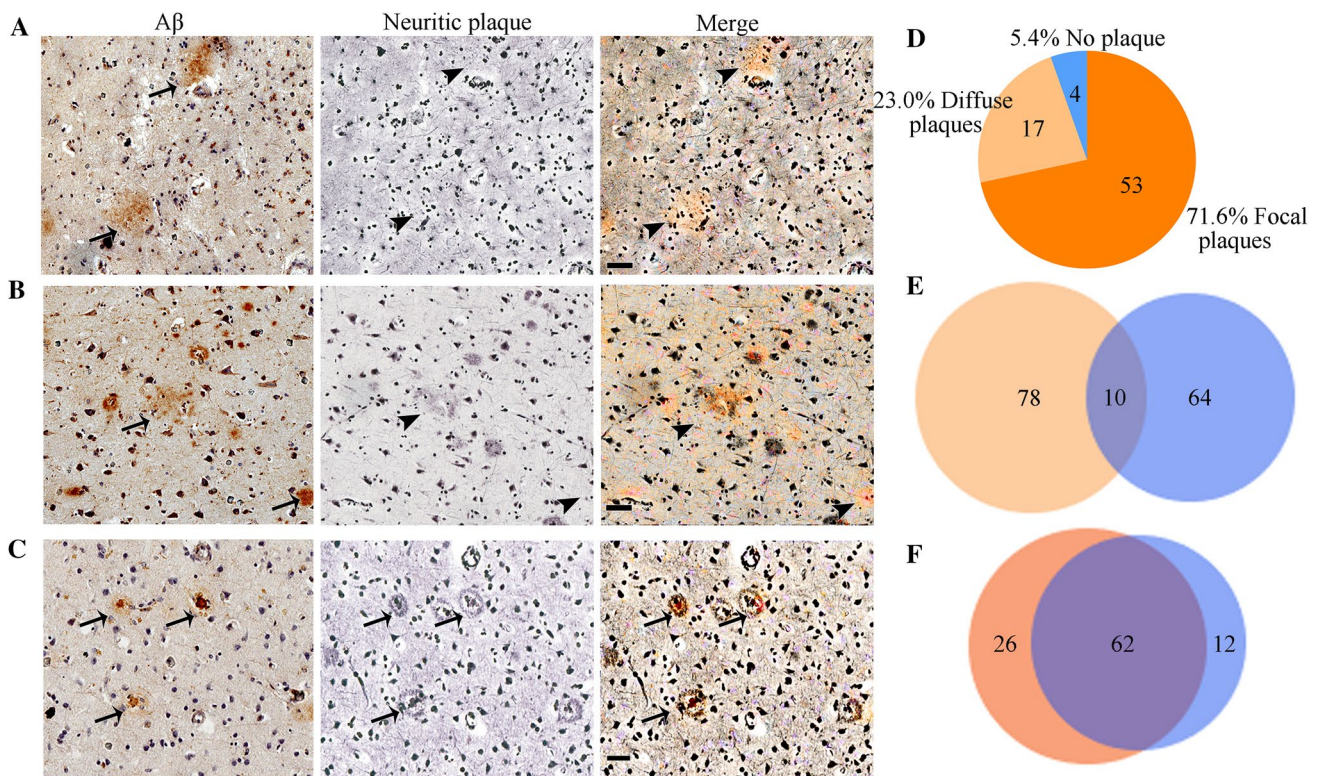


**Fig. 4** Correlation between different A $\beta$  plaque forms and neuritic plaques in the hippocampus. **A** Histochemical staining of diffuse A $\beta$  plaques and modified Bielschowsky staining of neuritic plaques in the hippocampus from the normal group. **B, C** Histochemical staining of diffuse (**B**) and focal (**C**) A $\beta$  plaques and modified Bielschowsky staining of neuritic plaques in the hippocampus from the AD group. **D** The coincidence rate of neuritic plaques and different A $\beta$  plaque forms. **E** The coincidence between diffuse A $\beta$  plaques and neuritic

plaques. A total of 11.4% of diffuse plaques coincided with neuritic plaques, and 13.5% of neuritic plaques coincided with diffuse plaques. **F** The coincidence between focal A $\beta$  plaques and neuritic plaques. A total of 70.5% of focal plaques coincided with neuritic plaques, and 83.8% of neuritic plaques coincided with focal plaques. In (**A–C**), the arrows show A $\beta$  plaques or neuritic plaques, and the arrowheads show no neuritic plaques. Scale bars, 50  $\mu$ m. In (**E–F**), yellow represents A $\beta$  plaques, and blue represents neuritic plaques.

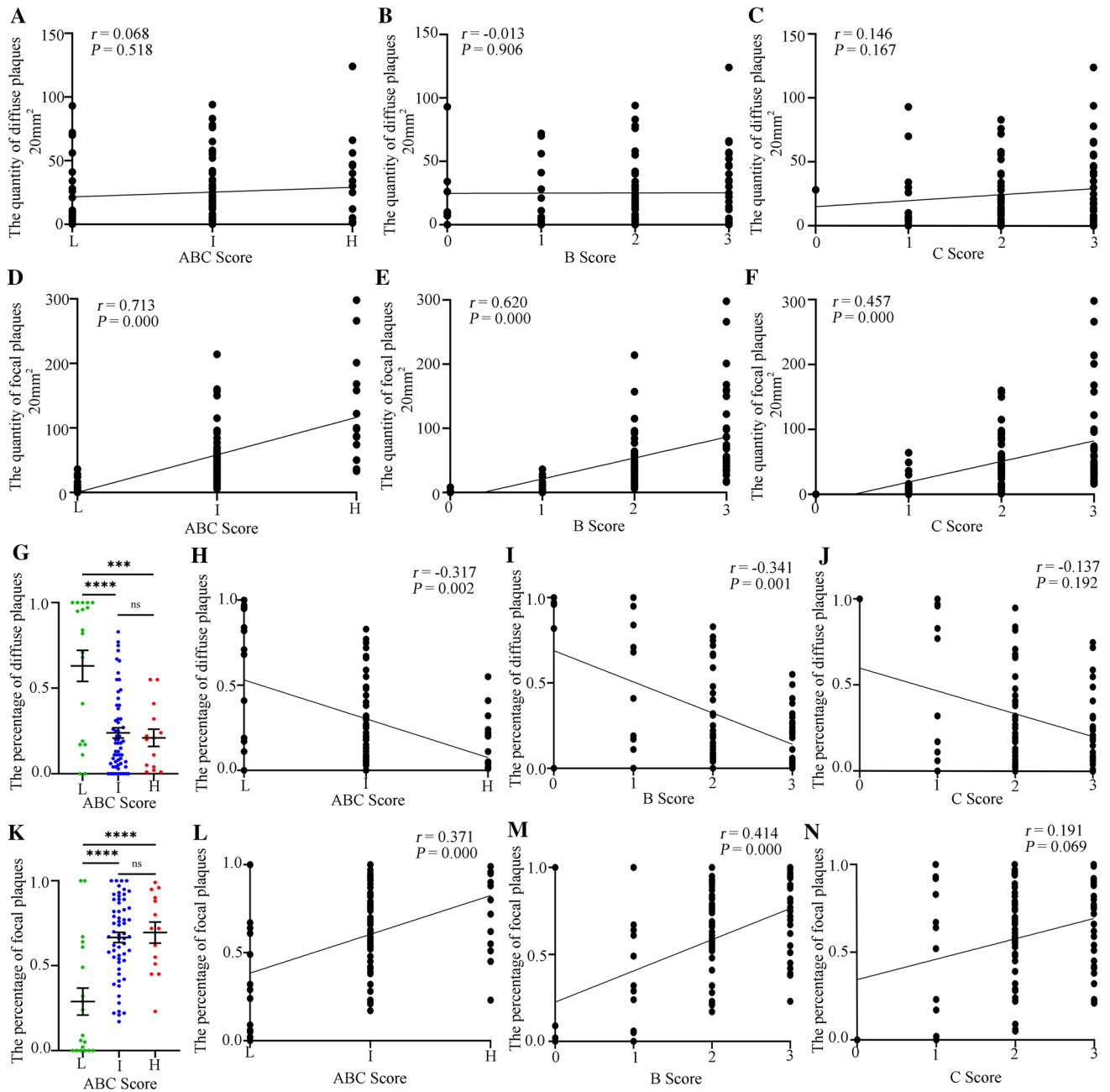


**Fig. 5** Correlations between ABC scores and different A $\beta$  plaque forms in the hippocampus. **A** Correlation between number of diffuse A $\beta$  plaques and ABC score. **B** Correlation between number of diffuse A $\beta$  plaques and B score. **C** Correlation between number of diffuse A $\beta$  plaques and C score. **D** Correlation between number of focal plaques and ABC score. **E** Correlation between number of focal plaques and B score. **F** Correlation between number of focal plaques and C score. **G** Percentage of diffuse A $\beta$  plaques in different ABC score groups. \*\*\*\* $P < 0.0001$ , \*\*\*\* $P < 0.0001$ , ns, no significant difference, by one-way ANOVA followed by Scheffe's *post-hoc* test. **H** Correlation between ABC score and the percentage of diffuse A $\beta$  plaques.  $P < 0.05$  for significance,  $r = -0.317$  for negative correlation, by Spearman correlation. **I** Correlation between B score and the percentage of diffuse A $\beta$  plaques.  $P < 0.05$  for significance,  $r = -0.341$  for negative correlation,

by Spearman correlation. **J** Correlation between C score and percentage of diffuse A $\beta$  plaques. **K** Percentage of focal A $\beta$  plaques in different ABC score groups. \*\*\*\* $P < 0.0001$ , ns, no significant difference by one-way ANOVA followed by Scheffe's *post-hoc* test. **L** Correlation between ABC score and percentage of focal A $\beta$  plaques.  $P < 0.05$  for significance,  $r = 0.371$  for positive correlation by Spearman correlation. **M** Correlation between B score and percentage of focal A $\beta$  plaques.  $P < 0.05$  for significance,  $r = 0.414$  for positive correlation by Spearman correlation. **N** Correlation between C score and percentage of focal A $\beta$  plaques. In (A–N), L group = 19 samples, I group = 59 samples, and H group = 14 samples.  $P < 0.05$  for significance,  $r > 0.5$  for positive correlation by Spearman correlation.

### The Association Between Hippocampal A $\beta$ Plaque Forms and Cognitive Dysfunction

Spearman correlation analysis was used to further confirm the relationship between different A $\beta$  plaque forms in the hippocampus and cognitive dysfunction. The number of focal A $\beta$  plaques, but not diffuse A $\beta$  plaques, had a significantly positive correlation with the ECog score (Fig. 6A, B). However, the percentages of neither diffuse nor focal A $\beta$  plaques showed significant correlation with the ECog score (Fig. 6C, D).

### The Association Between Hippocampal A $\beta$ Plaque Forms and Neuroinflammation

The pathological changes of AD are closely correlated with neuroinflammation [41]. Immunostaining showed that the focal A $\beta$  plaques were surrounded by more microglia

than diffuse A $\beta$  plaques in the hippocampus (Fig. 7A, B). Fifty plaques from 6 samples covering the “L/I/H” groups for each type were randomly selected, and the statistical results showed significantly more focal plaques coincided with IBA1-positive cells than diffuse plaques (Fig. 7C). CD68 is a heavily glycosylated glycoprotein that is strongly expressed in macrophages and other mononuclear phagocytes, including microglia. The relationship between CD68-positive cells and different types of plaque was similar to that of IBA1 (Fig. 7E–F), further showing that microglia are preferentially attracted by focal rather than diffuse A $\beta$  plaques. We also co-labeled different types of A $\beta$  plaque with CD86 and CD19. CD86 is a transmembrane glycoprotein that is constitutively expressed on memory B cells, germinal center B cells, and macrophages. In addition, CD86 is expressed at low levels on microglia and is upregulated through interferon- $\gamma$  stimulation. Our results showed that focal, but not diffuse A $\beta$  plaques strongly overlapped

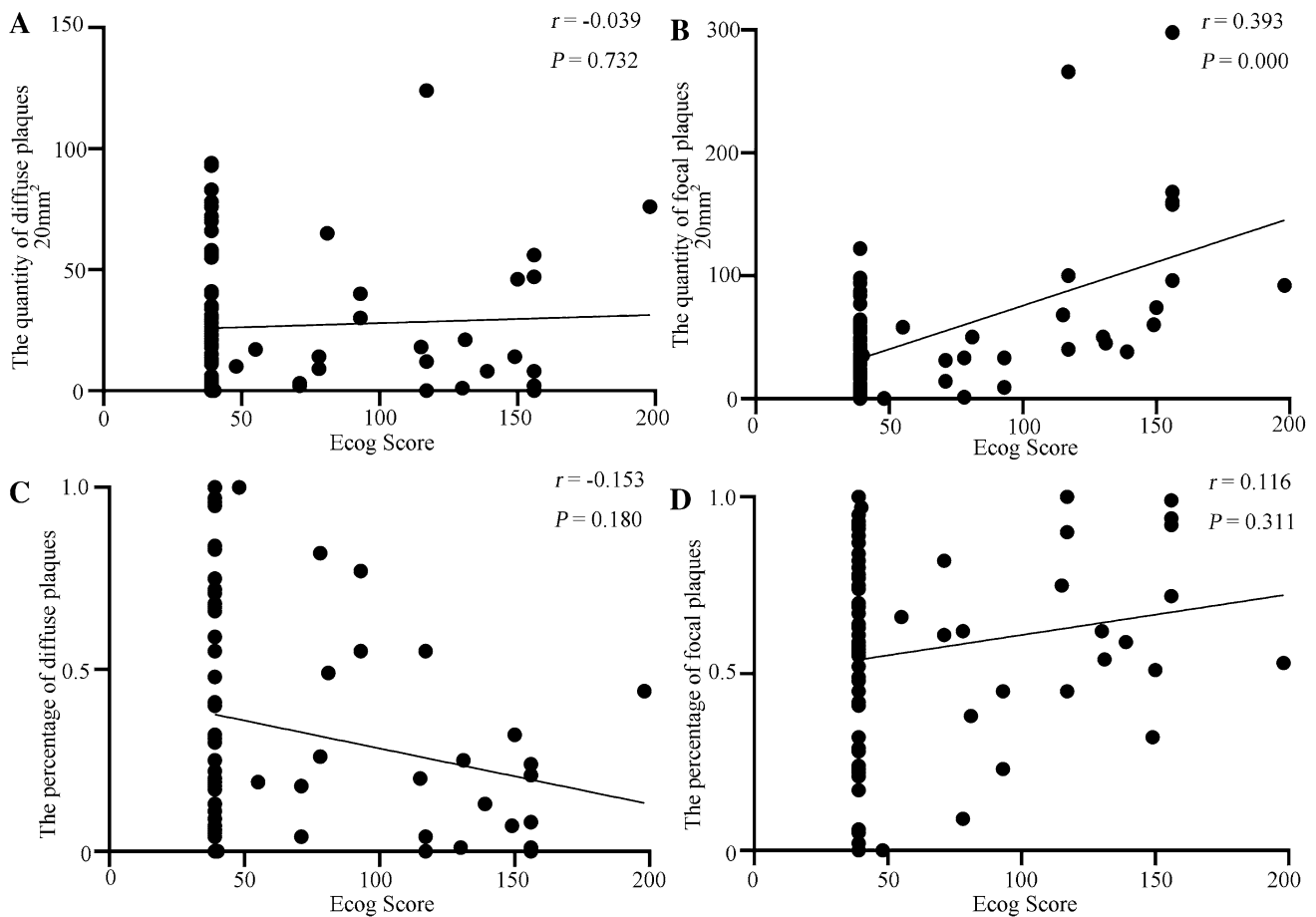


**Fig. 6** Correlations between ECog scores and the different A $\beta$  plaque forms in the hippocampus. **A** Correlation between number of diffuse A $\beta$  plaques and ECog score. **B** Correlation between number of focal A $\beta$  plaques and ECog score.  $P < 0.05$  for signifi-

cance,  $r = 0.393$  for positive correlation by Spearman correlation. **C** Correlation between diffuse A $\beta$  plaque percentage and ECog score. **D** Correlation between focal A $\beta$  plaque percentage and ECog score.

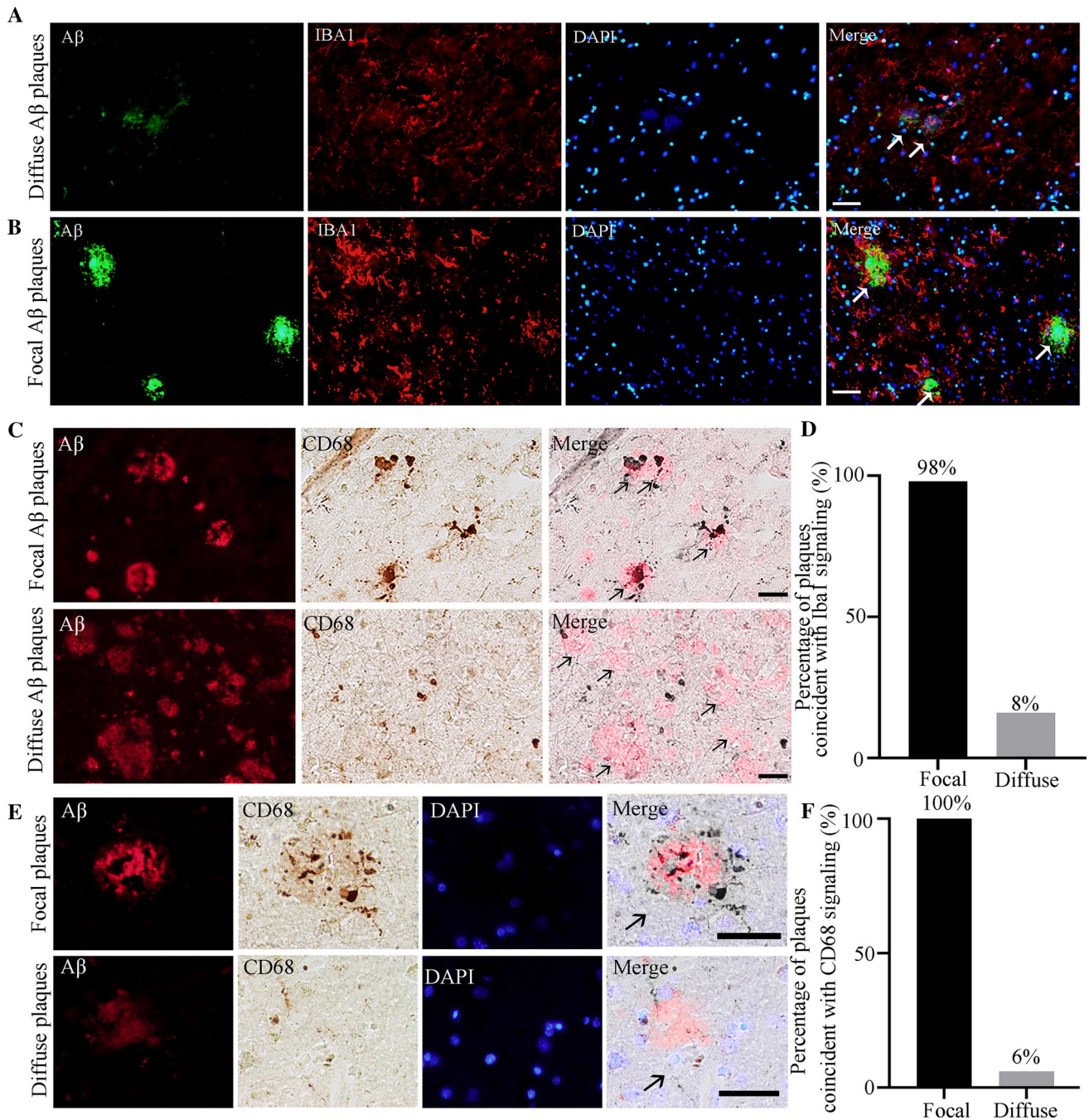


**Fig. 7** Relationships between microglial cells and the different Aβ plaque forms in the hippocampus. **A** Representative images of double immunostaining for diffuse Aβ plaques, IBA1, and DAPI. **B** Representative images of double immunostaining for focal Aβ plaques, IBA1, and DAPI. **C** Representative images of double immunostaining for different types of Aβ plaque and CD68. **E** Representative images

of double immunostaining for focal Aβ plaques, CD68, and DAPI. Scale bars, 50 μm in (A–C) and (E). **D**, **F** Percentages of different types of plaques coincident with IBA1- (**D**) and CD68-positive (**F**) cells.  $n = 50$  for each plaque type in the hippocampus from 6 human brain samples covering the “L/I/H” group.

with CD86-positive cells (Fig. 8A, C, D). Fifty randomly-selected focal plaques all coincided with CD86-positive cells, while no diffuse plaque coincided with CD86-positive cells (Fig. 8B). CD19 is a leukocyte differentiation antigen expressed by B cells belonging to the Ig superfamily.

Double immunostaining showed that more CD19-positive cells were found near the focal plaques than the diffuse plaques (Fig. 8E–H). This demonstrated that, in addition to microglia, focal Aβ plaques also attract B cells or other inflammatory cells to a certain extent.

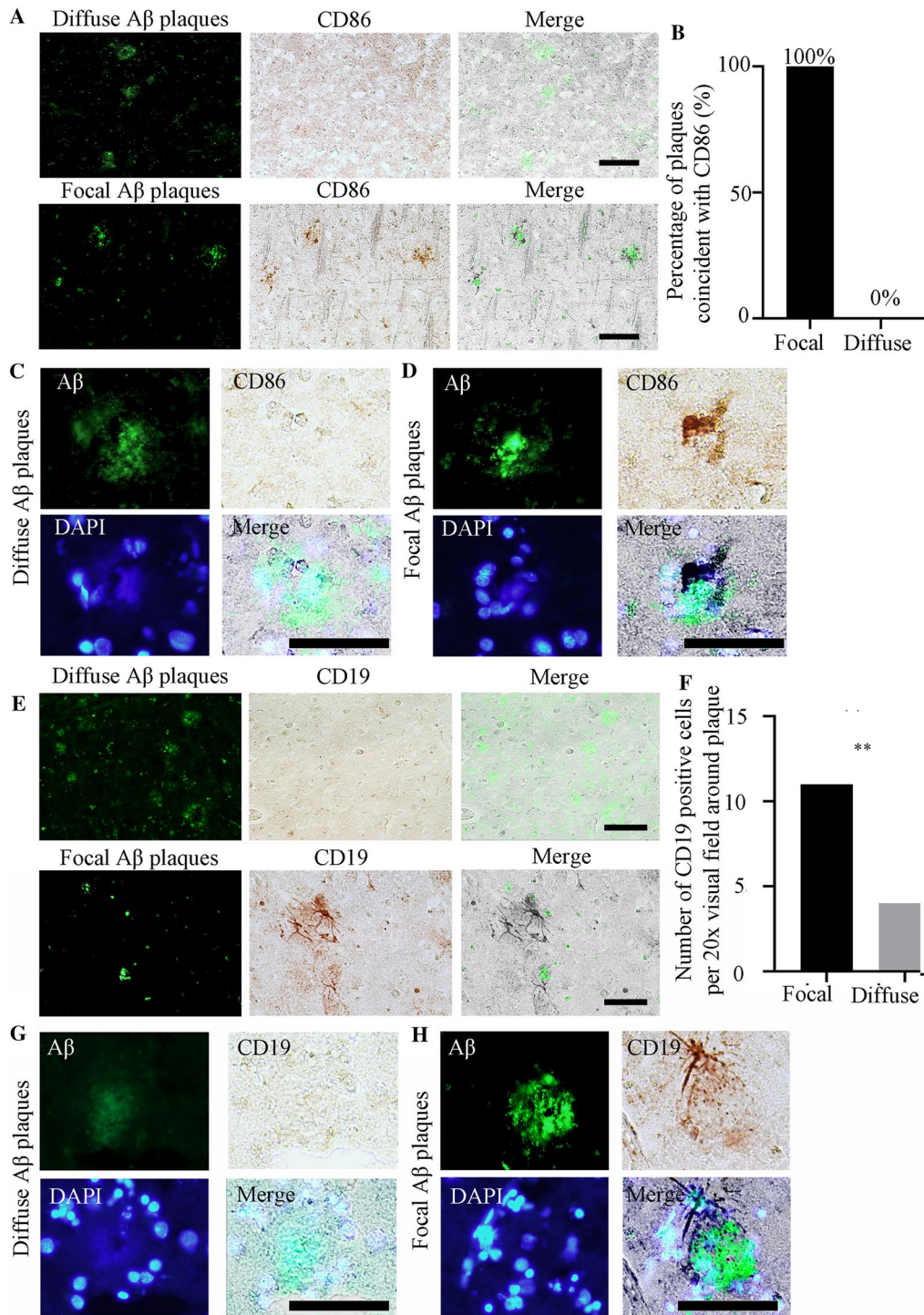


**Fig. 8** Relationships between CD86- or CD19-positive cells and A $\beta$  plaque formation in the hippocampus. **A** Representative images of double immunostaining for different types of A $\beta$  plaque and CD86. **B** Percentages of different types of plaques coincident with CD86-positive cells.  $n = 50$  per plaque type from 6 human brain samples covering the “L/I/H” group. **C** Representative images of double immunostaining for diffuse A $\beta$  plaques, CD86, and DAPI. **D** Representative images of double immunostaining for focal A $\beta$  plaques, CD86, and DAPI. **E** Representative images of double immunostaining for differ-

ent types of A $\beta$  plaque and CD19. **F** Number of CD19-positive cells per 20 $\times$  visual field around different types of A $\beta$  plaque.  $n = 50$  per plaque type in 6 human brain samples covering the “L/I/H” group. **G** Representative images of double immunostaining for diffuse A $\beta$  plaque, CD19, and DAPI. **H** Representative images of double immunostaining for different types of focal A $\beta$  plaque, CD19, and DAPI. Scale bars, 50  $\mu$ m in (A), (C), (D), (E), (G), and (H).

## Discussion

The neuropathological changes in AD are ranked along three parameters – A $\beta$  plaque score, Braak NFT stage, and CERAD NP score – to obtain an ABC score [36]. The A score reveals the distribution of A $\beta$  deposits in separate brain regions, and the C score reflects the density of cortical NPs [36], while the B score reveals the distribution of NFTs, which initially appear in the entorhinal cortex and then diffuse to the hippocampus and neocortex [42]. Several pieces of evidence suggest that NFTs may be the main driver of neurodegeneration in AD, and only when tau spreads from the entorhinal cortex into the neocortex can cognitive impairment be noted [43–45]. Although early studies have revealed that the accumulation of A $\beta$  plaques enhances the formation and progression of tau pathology and NPs, it is not fully clear which specific A $\beta$  plaque types are involved. Many studies have shown a lack of correlation between A $\beta$  plaques and cognitive decline in AD patients [20–22]. In particular, our previous study reported that the C score had a significant correlation with the ECog score, while the A score had no significant correlation with any of the ECog domains, indicating that more comprehensive and detailed analysis of A $\beta$  pathology was needed [22]. In the present study, we specifically assessed the relationship between morphologically different forms of A $\beta$  plaque and the pathological changes in AD. We researched the correlation between different A $\beta$  plaque forms in the hippocampus and ABC score, B score, or C score, and found that the number of focal plaques was positively correlated with the three scores. Moreover, the overwhelming majority of focal plaques coincided with NPs of the C score, while diffuse plaques did not. Our results showed that the more focal A $\beta$  plaques in the hippocampus, the worse was the general AD neuropathology, while there was no relationship between the quantity of diffuse plaques and the severity of neuropathological changes in AD. Further calculating the percentages of focal and diffuse plaques, the percentage of focal plaques was still positively correlated with the ABC score and B score, and the percentage of diffuse plaques changed to become negatively correlated with these two scores. These results further suggest that focal plaques in the hippocampus may contribute to the neuropathological changes in AD. However, follow-up experiments are needed to further determine whether the amyloid plaques in older individuals and AD patients with severe pathological symptoms are larger and thus harbor larger cores. Whether human brains were accurately derived from familial or sporadic AD patients is also needed for research. Symptomatic AD follows an insidious and progressive course, which is characterized by early impairment in learning and memory, followed by later impairments in complex attention, executive function, language, visuospatial function, praxis, gnosis, and behavior and/or social abnormalities [46]. Here, we found that the

number of focal A $\beta$  plaques was positively correlated with the ECog score. Diffuse plaques had no correlation with the ECog score. Our results demonstrate that focal plaques rather than diffuse plaques in the hippocampus can predict the cognitive level to some extent.

Microglia are primary inflammatory cells in the brain. Activated microglia are characterized by morphological and functional changes, including but not limited to increased phagocytosis and increased expression of receptors, cytokines, chemokines, and additional inflammation-related molecules [47]. Reactive glial cells occur within neuritic plaques, and further studies have shown that both reactive astrocytes and microglia occur in the vicinity of A $\beta$  plaques [35, 48]. Reactive glia and associated neuroinflammation are now regarded as playing key roles in both disease initiation and progression [35, 41, 47]. Our findings revealed that there were always a considerable number of microglia around the focal plaques in the hippocampus, while diffuse plaques had a poor ability to attract these microglia. This phenomenon indicates that focal rather than diffuse A $\beta$  plaques in the hippocampus are strongly correlated with neuroinflammation. We also co-localized different types of A $\beta$  plaque with CD19, a leukocyte differentiation antigen expressed by B cells, to research the relationship between A $\beta$  plaques and B lymphocytes. As in a previous study, B lymphocytes in the central nervous system were mostly located in the meninges and cerebrospinal fluid [49–51]. Our results showed that there were also B lymphocytes in the brain parenchyma, and there were more B lymphocytes near focal plaques than diffuse plaques, suggesting the regulatory mechanism of the adaptive immune response in focal A $\beta$  neuropathology. These findings suggest that the adaptive immune response in the central nervous system may be involved in the pathogenesis and development of AD neuropathology.

There is a view that diffuse plaques form earlier from the accumulation of amyloid-beta and then evolve over time into dense-core plaques. This model also emphasizes that extracellular amyloid is pathological and leads to inflammation. This model, however, does not adequately explain the occurrence or fate of intraneuronal amyloid, nor does it reveal any relation between the intraneuronal amyloid burden and amyloid plaques. Much experimental evidence has shown that there are different origins of amyloid plaques in the human brain. Diffuse plaques do not contain neuron-derived DNA or cytoplasmic proteins, have nothing to do with neuronal death and lysis, and do not seem to affect local axons or dendrites. Focal plaques contain the residue released by cell lysis after neuronal necrosis, and this surrounds the dense core usually containing neuronal nuclei in the form of spherical clouds. Various staining results have shown that the dense core of focal plaques has a certain resistance to the proteolysis of lysosomal enzymes released during neuronal lysis; they are proteolysis-resistant proteins. Centromeric

sequences found in focal plaques represent residual DNA fragments, which are dispersed in plaques after neuronal nuclear degradation [30]. The presence of neuron-derived focal plaques can easily explain the relationship between the increase in A $\beta$  plaques and the decrease in neurons in the cerebral cortex in AD [52]. Our study demonstrates that the number of focal plaques rather than diffuse plaques is associated with more severe cognitive impairment and inflammatory infiltration, and it is more toxic, which further supports the view of different origins. Moreover, the A $\beta$  components of different types of plaque are different. A $\beta$ 42 is the main component of plaques, and its aggregation rate is faster than that of A $\beta$ 40 [53]. Diffuse plaques and loosely-packed focal plaque material mainly consist of filamentous A $\beta$ 42, whereas plaque cores are made of both A $\beta$ 40 and A $\beta$ 42.

The neuropathological changes in AD are associated with focal A $\beta$  plaques rather than diffuse A $\beta$  plaques in the hippocampus. More importantly, focal A $\beta$  plaques rather than all forms of plaque in the hippocampus are positively correlated with recognition dysfunction. Moreover, compared to diffuse A $\beta$  plaques, focal A $\beta$  plaques are more associated with neuroinflammation, regardless of the innate immune response or adaptive immune response.

**Acknowledgements** This work was supported by grants from the National Natural Science Foundation of China (81771205 and 81801114), the CAMS Innovation Fund for Medical Sciences (2021-I2M-1-025), and Science Innovation 2030–Brain Science and Brain-Inspired Intelligence Technology Major Project (2021ZD0201100 and 2021ZD0201101). We thank Dr. Xiaojin Qian and Dr. Yongmei Chen (Department of Anatomy, Histology and Embryology, Institute of Basic Medical Sciences, Chinese Academy of Medical Sciences) for technical assistance in immunohistochemistry.

**Conflict of interest** There are no potential conflicts in the financial and material support for this research.

**Open Access** This article is licensed under a Creative Commons Attribution 4.0 International License, which permits use, sharing, adaptation, distribution and reproduction in any medium or format, as long as you give appropriate credit to the original author(s) and the source, provide a link to the Creative Commons licence, and indicate if changes were made. The images or other third party material in this article are included in the article's Creative Commons licence, unless indicated otherwise in a credit line to the material. If material is not included in the article's Creative Commons licence and your intended use is not permitted by statutory regulation or exceeds the permitted use, you will need to obtain permission directly from the copyright holder. To view a copy of this licence, visit <http://creativecommons.org/licenses/by/4.0/>.

## References

1. Condello C, Yuan P, Schain A, Grutzendler J. Microglia constitute a barrier that prevents neurotoxic protofibrillar A $\beta$ 42 hotspots around plaques. *Nat Commun* 2015, 6: 6176.
2. Haass C, Kaether C, Thinakaran G, Sisodia S. Trafficking and proteolytic processing of APP. *Cold Spring Harb Perspect Med* 2012, 2: a006270.
3. Wei W, Nguyen LN, Kessels HW, Hagiwara H, Sisodia S, Malinow R. Amyloid beta from axons and dendrites reduces local spine number and plasticity. *Nat Neurosci* 2010, 13: 190–196.
4. Verges DK, Restivo JL, Goebel WD, Holtzman DM, Cirrito JR. Opposing synaptic regulation of amyloid- $\beta$  metabolism by NMDA receptors *in vivo*. *J Neurosci* 2011, 31: 11328–11337.
5. Cirrito JR, Kang JE, Lee J, Stewart FR, Verges DK, Silverio LM. Endocytosis is required for synaptic activity-dependent release of amyloid-beta *in vivo*. *Neuron* 2008, 58: 42–51.
6. Leyns CEG, Gratuze M, Narasimhan S, Jain N, Koscal LJ, Jiang H, *et al.* TREM2 function impedes tau seeding in neuritic plaques. *Nat Neurosci* 2019, 22: 1217–1222.
7. Holtzman DM, Morris JC, Goate AM. Alzheimer's disease: The challenge of the second century. *Sci Transl Med* 2011, 3: 77sr1. <https://pubmed.ncbi.nlm.nih.gov/21471435/>
8. Chen ZC, Zhong CJ. Oxidative stress in Alzheimer's disease. *Neurosci Bull* 2014, 30: 271–281.
9. Liu Y, Wu G, Shu XJ, Wang XC. Targeting the transnitrosylation cascade provides a novel therapeutic strategy for Alzheimer's disease. *Neurosci Bull* 2021, 37: 1373–1376.
10. Selkoe DJ, Hardy J. The amyloid hypothesis of Alzheimer's disease at 25 years. *EMBO Mol Med* 2016, 8: 595–608.
11. Pooler AM, Polydoro M, Maury EA, Nicholls SB, Reddy SM, Wegmann S, *et al.* Amyloid accelerates tau propagation and toxicity in a model of early Alzheimer's disease. *Acta Neuropathol Commun* 2015, 3: 14.
12. Hurtado DE, Molina-Porcel L, Iba M, Aboagye AK, Paul SM, Trojanowski JQ, *et al.* A $\beta$  accelerates the spatiotemporal progression of tau pathology and augments tau amyloidosis in an Alzheimer mouse model. *Am J Pathol* 2010, 177: 1977–1988.
13. Hashimoto K, Iyo M. Amyloid cascade hypothesis of Alzheimer's disease and alpha 7 nicotinic receptor. *Nihon Shinkei Seishin Yakurigaku Zasshi* 2002, 22: 49–53.
14. Bedner P, Dupper A, Hüttmann K, Müller J, Herde MK, Dublin P, *et al.* Astrocyte uncoupling as a cause of human temporal lobe epilepsy. *Brain* 2015, 138: 1208–1222.
15. Hardy JA, Higgins GA. Alzheimer's disease: The amyloid cascade hypothesis. *Science* 1992, 256: 184–185.
16. Linse S, Scheidt T, Bernfur K, Vendruscolo M, Dobson CM, Cohen SIA, *et al.* Kinetic fingerprints differentiate the mechanisms of action of anti-A $\beta$  antibodies. *Nat Struct Mol Biol* 2020, 27: 1125–1133.
17. Van Dyck CH. Anti-amyloid- $\beta$  monoclonal antibodies for Alzheimer's disease: Pitfalls and promise. *Biol Psychiatry* 2018, 83: 311–319.
18. Pleen J, Townley R. Alzheimer's disease clinical trial update 2019–2021. *J Neurol* 2022, 269: 1038–1051.
19. Jeremic D, Jiménez-Díaz L, Navarro-López JD. Past, present and future of therapeutic strategies against amyloid- $\beta$  peptides in Alzheimer's disease: A systematic review. *Ageing Res Rev* 2021, 72: 101496.
20. Long JM, Holtzman DM. Alzheimer disease: An update on pathobiology and treatment strategies. *Cell* 2019, 179: 312–339.
21. Hara Y, McKeenan N, Fillit HM. Translating the biology of aging into novel therapeutics for Alzheimer disease. *Neurology* 2019, 92: 84–93.
22. Qiu WY, Yang Q, Zhang WY, Wang NL, Zhang D, Huang Y, *et al.* The correlations between postmortem brain pathologies and cognitive dysfunction in aging and Alzheimer's disease. *Curr Alzheimer Res* 2018, 15: 462–473.
23. Xiong F, Ge W, Ma C. Quantitative proteomics reveals distinct composition of amyloid plaques in Alzheimer's disease. *Alzheimers Dement* 2019, 15: 429–440.
24. O'Dell RS, Mecca AP, Chen MK, Naganawa M, Toyonaga T, Lu Y, *et al.* Association of A $\beta$  deposition and regional synaptic density in early Alzheimer's disease: A PET imaging study with [<sup>11</sup>C]UCB-J. *Alzheimers Res Ther* 2021, 13: 11.

25. Hwang JY, Byun MS, Choe YM, Lee JH, Yi D, Choi JW, *et al.* Moderating effect of *APOE*  $\epsilon$ 4 on the relationship between sleep-wake cycle and brain  $\beta$ -amyloid. *Neurology* 2018, 90: e1167–e1173.
26. Sengupta U, Nilson AN, Kaye R. The role of amyloid- $\beta$  oligomers in toxicity, propagation, and immunotherapy. *EBioMedicine* 2016, 6: 42–49.
27. Kwak SS, Washicosky KJ, Brand E, von Maydell D, Aronson J, Kim S, *et al.* Amyloid- $\beta$ 42/40 ratio drives tau pathology in 3D human neural cell culture models of Alzheimer's disease. *Nat Commun* 2020, 11: 1377.
28. Suire CN, Abdul-Hay SO, Sahara T, Kang D, Brizuela MK, Saftig P, *et al.* Cathepsin D regulates cerebral A $\beta$ 42/40 ratios *via* differential degradation of A $\beta$ 42 and A $\beta$ 40. *Alzheimers Res Ther* 2020, 12: 80.
29. Wisniewski T, Konietzko U. Amyloid-beta immunisation for Alzheimer's disease. *Lancet Neurol* 2008, 7: 805–811.
30. D'Andrea MR, Nagele RG. Morphologically distinct types of amyloid plaques point the way to a better understanding of Alzheimer's disease pathogenesis. *Biotech Histochem* 2010, 85: 133–147.
31. D'Andrea MR, Cole GM, Ard MD. The microglial phagocytic role with specific plaque types in the Alzheimer disease brain. *Neurobiol Aging* 2004, 25: 675–683.
32. Bussi ere T, Bard F, Barbour R, Grajeda H, Guido T, Khan K, *et al.* Morphological characterization of thioflavin-S-positive amyloid plaques in transgenic alzheimer mice and effect of passive a $\beta$  immunotherapy on their clearance. *Am J Pathol* 2004, 165: 987–995.
33. Gouras GK, Tampellini D, Takahashi RH, Capetillo-Zarate E. Intraneuronal beta-amyloid accumulation and synapse pathology in Alzheimer's disease. *Acta Neuropathol* 2010, 119: 523–541.
34. Takahashi RH, Almeida CG, Kearney PF, Yu FM, Lin MT, Milner TA, *et al.* Oligomerization of Alzheimer's beta-amyloid within processes and synapses of cultured neurons and brain. *J Neurosci* 2004, 24: 3592–3599.
35. Keren-Shaul H, Spinrad A, Weiner A, Matcovitch-Natan O, Dvir-Szternfeld R, Ulland TK, *et al.* A unique microglia type associated with restricting development of Alzheimer's disease. *Cell* 2017, 169: 1276–1290.e17.
36. Montine TJ, Phelps CH, Beach TG, Bigio EH, Cairns NJ, Dickson DW, *et al.* National Institute on Aging-Alzheimer's Association guidelines for the neuropathologic assessment of Alzheimer's disease: A practical approach. *Acta Neuropathol* 2012, 123: 1–11.
37. Farias ST, Park LQ, Harvey DJ, Simon C, Reed BR, Carmichael O, *et al.* Everyday cognition in older adults: Associations with neuropsychological performance and structural brain imaging. *J Int Neuropsychol Soc* 2013, 19: 430–441.
38. Marshall GA, Zoller AS, Kelly KE, Amariglio RE, Locascio JJ, Johnson KA, *et al.* Everyday cognition scale items that best discriminate between and predict progression from clinically normal to mild cognitive impairment. *Curr Alzheimer Res* 2014, 11: 853–861.
39. Suenaga T, Hirano A, Llana JF, Yen SH, Dickson DW. Modified Bielschowsky stain and immunohistochemical studies on striatal plaques in Alzheimer's disease. *Acta Neuropathol* 1990, 80: 280–286.
40. Roy S. *Neuropathology: a reference text of CNS pathology*. 2nd edition. David Ellison, Seth Love, Leila Chimelli, Brian N. Harding, James Lowe, and Harry V. Vinters, 754 pp, \$365. *Hum Pathol* 2005, 36: 224.
41. Leng FD, Edison P. Neuroinflammation and microglial activation in Alzheimer disease: Where do we go from here? *Nat Rev Neurol* 2021, 17: 157–172.
42. Goedert M. NEURODEGENERATION. Alzheimer's and Parkinson's diseases: The prion concept in relation to assembled A $\beta$ , tau, and  $\alpha$ -synuclein. *Science* 2015, 349: 1255–1255.
43. Giannakopoulos P, Herrmann FR, Bussi ere T, Bouras C, Kovari E, Perl DP, *et al.* Tangle and neuron numbers, but not amyloid load, predict cognitive status in Alzheimer's disease. *Neurology* 2003, 60: 1495–1500.
44. Nelson PT, Alafuzoff I, Bigio EH, Bouras C, Braak H, Cairns NJ, *et al.* Correlation of Alzheimer disease neuropathologic changes with cognitive status: A review of the literature. *J Neuropathol Exp Neurol* 2012, 71: 362–381.
45. Price JL, McKeel DW Jr, Buckles VD, Roe CM, Xiong CJ, Grundman M, *et al.* Neuropathology of nondemented aging: Presumptive evidence for preclinical Alzheimer disease. *Neurobiol Aging* 2009, 30: 1026–1036.
46. McKhann GM, Knopman DS, Chertkow H, Hyman BT, Jack CR Jr, Kawas CH, *et al.* The diagnosis of dementia due to Alzheimer's disease: Recommendations from the National Institute on Aging-Alzheimer's Association workgroups on diagnostic guidelines for Alzheimer's disease. *Alzheimers Dement* 2011, 7: 263–269.
47. Wolf SA, Boddeke HWGM, Kettenmann H. Microglia in physiology and disease. *Annu Rev Physiol* 2017, 79: 619–643.
48. Pan RY, Ma J, Kong XX, Wang XF, Li SS, Qi XL, *et al.* Sodium rutin ameliorates Alzheimer's disease-like pathology by enhancing microglial amyloid- $\beta$  clearance. *Sci Adv* 2019, 5: eaau6328.
49. Lipton HL. B lineage cells in inflammatory central nervous system. *Ann Neurol* 2006, 60: 486–487.
50. Prinz M, Priller J. The role of peripheral immune cells in the CNS in steady state and disease. *Nat Neurosci* 2017, 20: 136–144.
51. Sabatino JJ Jr, Pr obstel AK, Zamvil SS. B cells in autoimmune and neurodegenerative central nervous system diseases. *Nat Rev Neurosci* 2019, 20: 728–745.
52. D'Andrea MR, Nagele RG, Wang HY, Peterson PA, Lee DH. Evidence that neurones accumulating amyloid can undergo lysis to form amyloid plaques in Alzheimer's disease. *Histopathology* 2001, 38: 120–134.
53. Yang Y, Arseni D, Zhang WJ, Huang M, L ovestam S, Schweighauser M, *et al.* Cryo-EM structures of amyloid- $\beta$  42 filaments from human brains. *Science* 2022, 375: 167–172.